Controlled Drug Delivery and Ophthalmic Applications

J. A. Ferreira,[a] P. de Oliveira,[b,*] and P. M. da Silva[c]
[a]CMUC-Department of Mathematics, University of Coimbra
[b]CMUC-Department of Mathematics, University of Coimbra
[c]Department of Physics and Mathematics, Coimbra Institute of Engineering

Original scientific paper
Received: May 2, 2012
Accepted: June 11, 2012

The goal of this paper is to present an overview of drug delivery from polymeric therapeutic lens to the anterior segment of the eye. Mathematical models that describe *in vitro* and *in vivo* drug delivery, from different types of lens, are presented. Healthy and pathological situations are addressed. Numerical simulations are included and compared with experimental results.

Key words:
Controlled drug delivery, effective time, therapeutic lens, mathematical model, partial differential equations

Introduction

Controlled drug delivery occurs when a polymer is combined with a drug in a such a way that the release profile is predefined. Conventional forms of drug delivery are based on tablets, eye drops, ointments and intravenous solutions. These delivery systems were characterized by an immediate and non controlled kinetics depending essentially on the properties of tissues to absorb drugs.In the last decades drug delivery devices have moved to more complex controlled systems. Advances in polymer science have led to the development of second generation drug-delivery systems which purpose is to maintain drug concentration in the blood or in target tissues at a desired value and during an extended period of time. The improvements in the properties of polymers, by combining different compounds and additives, the use of biodegradable polymers and the enhancement of diffusion processes come at the expense of more complex transport phenomena which are known to influence drug delivery rates.[1,2] The urgency for mathematical models in the area and the necessity for a predictive environment, avoiding costly *in vitro* experiments, become all the more relevant in light of the heightened focus on polymer-based drug-delivery devices. Also future drug delivery modelling work should consider drug transport in target tissues after its release from polymeric devices.

Efficient drug delivery to the eye is becoming increasingly vital with the development of new devices and the increasing prevalence of eye diseases, accompanying population ageing. In this paper we will present an overview of drug delivery from therapeutic lens to the anterior segment of the eye. The platforms we analyse and the models we present to simulate the drug release can be easily adapted to the case of transdermal drug delivery systems.

The eye is anatomically divided into the anterior and posterior segments with the lens-iris barrier roughly demarcating the two segments. For both the anterior and the posterior segment of the eye, topical route is very inefficient in delivering therapeutic concentrations because of drainage through the naso-lacrimal ducts, low permeability of corneal epithelium, systemic absorption and the blood aqueous barrier. According to these facts it is estimated that when a drop is instilled into the eye it is diluted by the lacrimal secretion and 95% is cleared by the tear fluid. To avoid drug loss, side effects and also to improve the efficiency of drug delivery, many researchers have proposed the use of therapeutic contact lenses as a vehicle to deliver ophthalmic drugs. The main advantage of this method is the possibility of controlling the drug delivery by means of the use of polymeric matrices designed to achieve pre-defined performances as well as their high degree of comfort and biocompatibility. Several techniques have been proposed in the literature. Without being exhaustive we can mention the use of

(i) soaked simple contact lenses;[3–5]

(ii) compound contact lenses with a hollow cavity;[6]

(iii) entrapment of drugs by polymerization of hydrogel monomers in the presence of species to be entrapped or by direct dissolution;[7–14]

(iv) biodegradable contact lenses.[15]

The use of soaked simple lens is more efficient than the use of ophthalmic drops but the drug loading is very limited and the delivery period of time is very short. In the case of lens with an hollow cavity it has been observed that the oxygen and carbon di-

*Corresponding author: P. de Oliveira, e-mail: poliveir@mat.uc.pt

oxide permeability is lower than the prescribed for a safe daily use. In the first of such papers the entrapment of the drug is achieved by polymerization of monomers and by encapsulation of drug within particles dispersed in the lens.[8,9] The nanoparticles are formed by polymerization, during or after which the drug is added, leading to covalent drug binding to the polymer. This binding of the drug depends on its physicochemical properties as well as the nature of the polymer. In the case of encapsulation in particles the drug to be delivered must overcome two barriers: the diffusion in the particles and the diffusion in the polymeric matrix. As a consequence the drug release attains in this case several days. The main difference between the two types of lens proposed [8,10] lies in the polymers used. In the first of such papers the polymeric matrix was made from a p-HEMA (Monomer 2-hydroxyethyl methacrylate) gel and the particles were stabilized with a silica shell; in the second of the previously mentioned papers the film was prepared using p-HEMA/MAA (Copolymer 2-hydroxyethyl methacrylate co-methacrylic acid) and silicone particles have been used. In the first case there is a delay period between the delivery from the polymeric matrix and from the particles. It can attain three or four days and during this period there is practically no drug delivery. In the second case the drug is continuously delivered with no pause period during the release.

At the best of our knowledge the more recent type of therapeutic lens has been proposed by a team of Harvard Medical School.[15] The idea underlying the mechanism used to induce a delay in the drug delivery is to use a sandwich type structure composed by three polymeric layers as represented in Figure 1: two non biodegradable layers (HEMA) coating a biodegradable PLGA (copolymer poly lactic co-glycolic acid) film containing drug. Numerical simulations of drug delivery from the lens with particles entrapping drug[10] and the sandwich lens[15] have been compared in a recent paper.[16] According to the numerical simulations presented there and to in *vitro* experiments[15] the release from the "sandwich lens" is slower than the release from therapeutic lens presented with particles entrapping drug,[8,10] lasting for thirty days.

From a medical point of view, the central question is to have a prediction of the drug concentration in the anterior chamber of the eye. In this case mathematical models are the only available tool to make such prediction. Several mathematical models describing the behaviour of drug concentration across the cornea when a drop is instilled can be found in the literature.[17–19] Nevertheless, when the drug is delivered from a contact lens the concentration and mass profiles across the cornea are qualitatively different as predicted by a mathematical model that simulates the concentration in the anterior chamber when the drug is delivered from a therapeutic contact lens, where the drug is dispersed in the polymeric matrix and encapsulated in nanoparticles.[11] A comparison with the behavior of concentration plots in the anterior chamber, in the case of topical drug administration, shows the efficiency of controlled drug delivery.

Therapeutic lens are essentially used in the case of severe diseases as glaucoma, for which long periods of drug delivery, from one week to a month, are needed. Glaucoma is related with a buildup of intraocular pressure (I.O.P.) due to an obstruction of Schlemm canals or an excessive production of aqueous humor (Figure 2). When the delivery in the anterior chamber is modelled by an ordinary differential equation, its anatomy is not taken into account.[11] To obtain a more realistic description of the delivery, the I.O.P. and the physio-pathological characteristics of the anterior chamber should be considered. To describe the *in vivo* delivery a mathematical model which consists of three coupled systems linked by interface conditions was considered: drug delivery from a therapeutic lens, diffusion and metabolic consumption in the cornea, diffusion, convection and metabolic consumption in the anterior chamber of the eye. Numerical simulations in healthy and pathological conditions can be of great help to ophthalmologists and to material scientists because they give indications of how to tailor polymeric lens to fit specific patient's needs.[20]

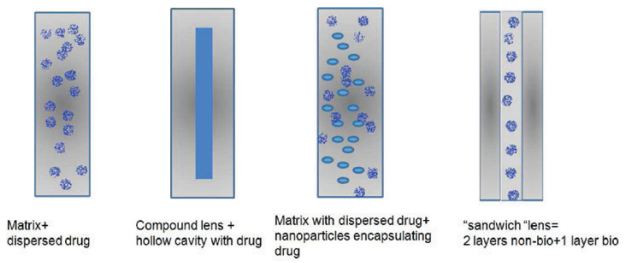

Fig. 1 – *Examples of single and multilayer drug delivery systems*

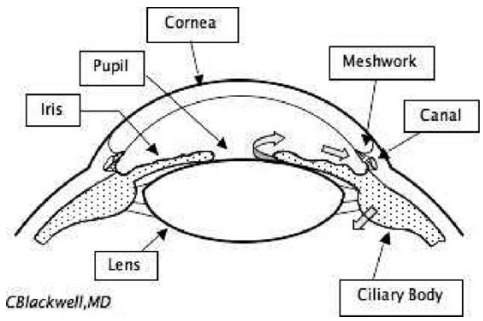

Fig. 2 – *Anatomy of the eye (http://www.blackwelleyesight.com/narrated-eye-exam/)*

We present two mathematical models that simulate *in vitro* drug delivery from the two different lenses.[10,15] Comparisons with laboratorial experiments are also presented. For the lens with particles a time constant which represents the mean time to achieve equilibrium – effective time[21,22] – is computed. A mathematical model that simulates *in vivo* drug delivery to the anterior chamber from a therapeutic lens is also presented.[20] Numerical simulations in healthy and pathological conditions are analysed. Finaly some conclusions are addressed.

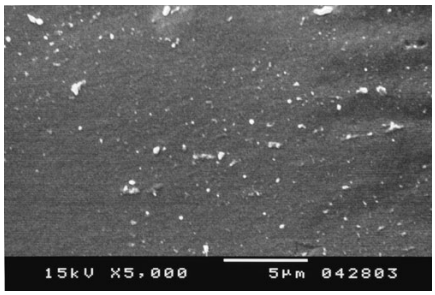

Fig. 3 – *SEM image of the cross section of a copolymer with particles*

Simulating *in vitro* drug release from therapeutic lens

In this Section we will focus mainly on two types of therapeutic lens: lens with dispersed particles encapsulating drug and sandwich type lens.[10,15]

Lens with particles

Mathematical model and laboratorial experiments

The lens is a p-HEMA/MAA platform with flurbiprofen dispersed and entrapping particles filled with drug.[10] The copolymers with drug incorporated in the polymeric matrix were synthesized by dissolving flurbiprofen directly into the mixture of monomers and adding a microemulsion containing silicone particles encapsulating drug. The solution was injected into a mold, constituted by two glass plates coated with teflon. The polymerization reaction was performed at 60 °C during 24 hours. The obtained copolymer was cut into circular samples with 1 cm of diameter.

In Figure 3 we present a SEM (scanning electron microscopy) micrograph of a copolymer with drug dispersed and particles encapsulating drug.[10]

The mathematical model used to simulate *in vitro* drug delivery (when the lens has a width of $2l$ and is completely immersed in water) which we denote by model I, is represented by the system of partial differential equations

$$\begin{cases} \dfrac{\partial C^g}{\partial t} = D\dfrac{\partial^2 C^g}{\partial x^2} - \dfrac{\partial C^b}{\partial t}, \quad x \in (-l,l), \quad t > 0 \\ \dfrac{\partial C^b}{\partial t} = \lambda(C^g - C^b), \quad x \in (-l,l), \quad t > 0 \end{cases} \tag{1}$$

where C^g represents the drug concentration in the gel, C^b the drug concentration in the particles, D the diffusion coefficient of the drug in the gel and λ stands for the product of the mass transfer coefficient for drug transport across the particle surface and the ratio between the surface and the volume of particles. We note that no diffusion was considered in the second equation in (1). The second equation in (1) is a good approximation of drug release from particles to the gel provided that the typical dimension of particles is small when compared with the size of lens. In this sense particles are looked as having no dimension, acting as immobilizing sites, and drug as having two states: free (C^g) and bound (C^b). We note that – except for what concerns Figures 12 and 13 – the units in the paper are presented in Annex A. The reason for such exception lies in the fact that the experimental plots exhibited in these Figures were in different units in the paper where a sandwich lens was first described.[15]

System (1) is completed with the initial conditions

$$\begin{cases} C^g(x,0) = C^{0g} \\ C^b(x,0) = C^{0b}, \end{cases} \tag{2}$$

where C^{0g} is the initial concentration in the gel and the C^{0b} the initial concentration inside the particles, and the boundary conditions

$$\begin{cases} C^g(-l,t) = C^E \\ C^g(l,t) = C^E, \end{cases} \tag{3}$$

with C^E representing an external concentration. Alternatively flux boundary conditions of type

$$\begin{cases} D\dfrac{\partial C^g}{\partial x}(-l,t) = \alpha_1(C^g(-l,t) - C^E), \quad t > 0 \\ -D\dfrac{\partial C^g}{\partial x}(l,t) = \alpha_1(C^g(l,t) - C^E), \quad t > 0 \end{cases} \tag{4}$$

can be considered, where α_1 stands for a transference coefficient. We note that (4) is a more realistic description of the clearance mechanisms, meaning that the drug flux at the boundary of the lens is proportional to the difference between the drug concentration in the exterior region and the drug concentration at the lens surface. Conditions (3) mean that the drug is immediately removed and the external drug concentration is constant. To simulate in laboratory this behaviour the concentration of drug in water is kept constant by means of a renewal mechanism that takes place at fixed intervals of time.

Due to the linearity of (1) an exact solution for the total released mass $M(t)$ can be computed. Using for a sake of simplicity conditions (3) we obtain after some tedious but straightforward computations[8]

$$M(t) = -\frac{4D}{l}\sum_{n=0}^{\infty}\frac{C^{E}(a_n + 2\lambda) - C^{0g}(a_n + \lambda) - \lambda C^{0b}}{a_n(a_n^2 + 2\lambda^2 + 2a_n\lambda)}(a_n + \lambda)(e^{a_n t} - 1), \tag{5}$$

where

$$a_n = \frac{-8\lambda l^2 - D(2n+1)^2\pi^2 \pm \sqrt{(8\lambda l^2)^2 + D^2(2n+1)^4\pi^4}}{8l^2}, \quad n = 0,1,\ldots$$

To have a clear picture of the delay effect of particles different scenario were considered (Table 1).

Table 1 – *Description of the Systems of Model I.*

Systems	Definition	Parameters
System 1	matrix with dispersed drug	$C^{0b} = 0,\ \lambda = 0$
System 2	matrix with silicone particles encapsulating drug	$C^{0g} = 0,\ \lambda \neq 0$
System 3	matrix with dispersed drug and entrapped in particles	$C^{0b} = C^{0g},\ \lambda \neq 0$
System 4	matrix with dispersed drug and void particles at $t = 0$	$C^{0b} = 0,\ \lambda \neq 0$

System 3 represents the lens with entrapped particles.[10] System 4 describes an academic situation used to test the robustness of the model.

Using $C^E = 0$ and the information in Table 1, it can be proved analytically, from (5) that for any choice of the parameters

$$M_2(t) < M_3(t) < M_4(t) < M_1(t), \quad t > 0, \tag{6}$$

where M_i, i = 1,2,3,4 represent the mass delivered from Systems 1, 2, 3 and 4 respectively. In Figure 4

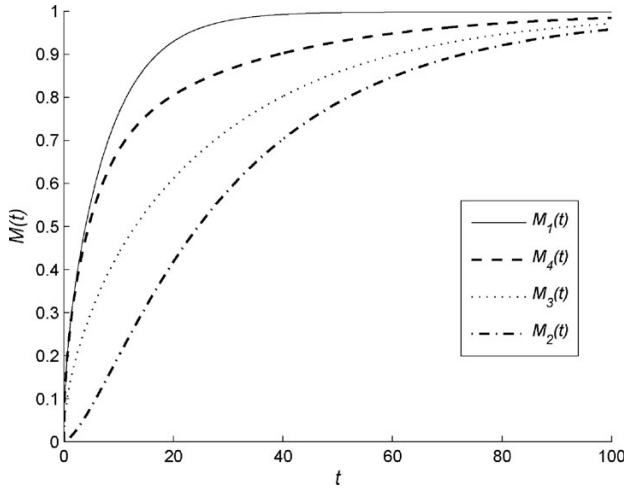

Fig. 4 – *Delay effect on the drug release of the particles for Systems 1, 2, 3 and 4*

we exhibit plots computed from the analytical solution (5) considering one hundred terms. We took $C^{0b} = 0.5$ for $M_2(t)$ and $C^{0g} = 0.5$ for $M_1(t)$ and $M_4(t)$. For $M_3(t)$ we considered $C^{0g} = C^{0b} = 0.25$. We note that the values of the parameters used in the simulations of Figure 4 are not physical.

In Figure 5 we exhibit experimental release profiles of flurbiprofen for Systems 1, 2 and 3 (S1, S2, S3). At this point we just want to underline the qualitative agrement between numerical results in Figure 4 and experimental results in Figure 5. In what follows physical parameters will be considered in the simulations.

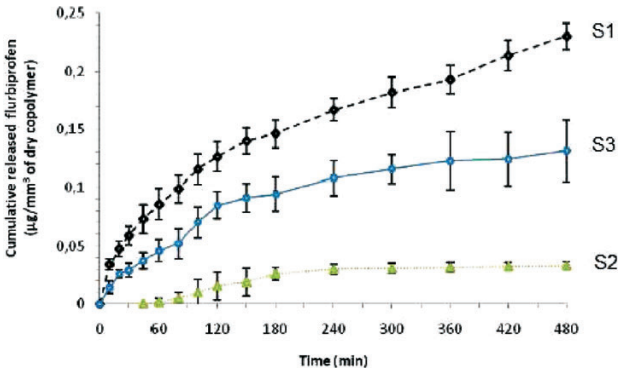

Fig. 5 – *Experimental release profiles of flurbiprofen for three different platforms*

Mean time to achieve equilibrium: effective time constant

To improve the design of the lens it is important to know the waiting time that is the period of time elapsed before the mass attains a certain therapeutic level and how to adjust the parameters to produce a pre-defined delivery profile. In this subsection we compute the effective time.[21]

Let Ms represents the steady mass that is $M^s = \lim_{t\to\infty} M(t)$. The effective time teff is defined as the mean time to achieve the equilibrium,

$$t_{eff} = \frac{\int_0^\infty t(M^s - M(t))\mathrm{d}t}{\int_0^\infty (M^s - M(t))\mathrm{d}t}, \qquad (7)$$

which can be seen as the first moment of the probability density function

$$d(t) = \frac{M^s - M(t)}{\int_0^\infty (M^s - M(t))\mathrm{d}t}. \qquad (8)$$

To compute t_{eff} only $\overline{M}(p)$, the Laplace transform of $M(t)$, must be known. In fact it can be proved[21,22] that if $\overline{M}(p)$ can be expanded in powers of p,

$$\overline{M}(p) = \frac{1}{p}(B_1 + B_2 p + B_3 p^2 + \dots), \qquad (9)$$

then

$$t_{eff} = -\frac{B_3}{B_2},$$

provided that $B_2 \neq 0$.

In the case $D \neq 0$, $\lambda \neq 0$, we give $\overline{M}(p)$ the form (9), with

$$B_1 = -2a\frac{l}{\lambda}, \quad B_2 = \frac{l}{\lambda}\left(\frac{a}{\lambda} + \frac{4a}{3D}l^2 - 2\varpi\right),$$

$$B_3 = \frac{l}{\lambda}\left(-\frac{4a}{3\lambda D}l^2 - \frac{16a}{15D^2}l^4 + \frac{2}{\varpi}\lambda + \frac{4\varpi}{3D}l^2 - \frac{a}{\lambda^2} + \frac{\varpi}{\lambda}\right),$$

where

$$a = 2\lambda C^E - \lambda(C^{0g} + C^{0b}), \quad \varpi = \frac{C^{0b} - C^{0g}}{2}.$$

After some tedious but straightforward computations we obtain[14]

$$t_{eff} = \frac{1}{\lambda D} \cdot \frac{2\varpi D^2\lambda - aD^2 - \frac{4}{3}a\lambda Dl^2 - \frac{16}{15}a\lambda^2 l^4 + \frac{4}{3}\varpi D\lambda^2 l^2}{2\varpi D\lambda - ad - \frac{4}{3}a\lambda l^2} \qquad (10)$$

In the case of System 1 ($\lambda = 0$, $C^{0b} = 0$), effective time can not be obtained from (10). A direct calculus from (9) leads to

$$t_{eff} = \frac{2l}{5D}. \qquad (11)$$

In Figure 6 plots of t_{eff} given by (10), as a function of λ and D, are exhibited with $C^{0g} = 0.5$, $C^{0b} = 0.25$, $C^E = 0$, $l = 1$. As expected effective time is a decreasing function of D, for constant λ, and a decreasing function of λ, for constant D. In fact when D increases the drug diffuses faster; when λ increases the drug encapsulated in the particles easier surmounts the barrier represented by their boundary. We note that the influence of D is more significant than the influence of λ.

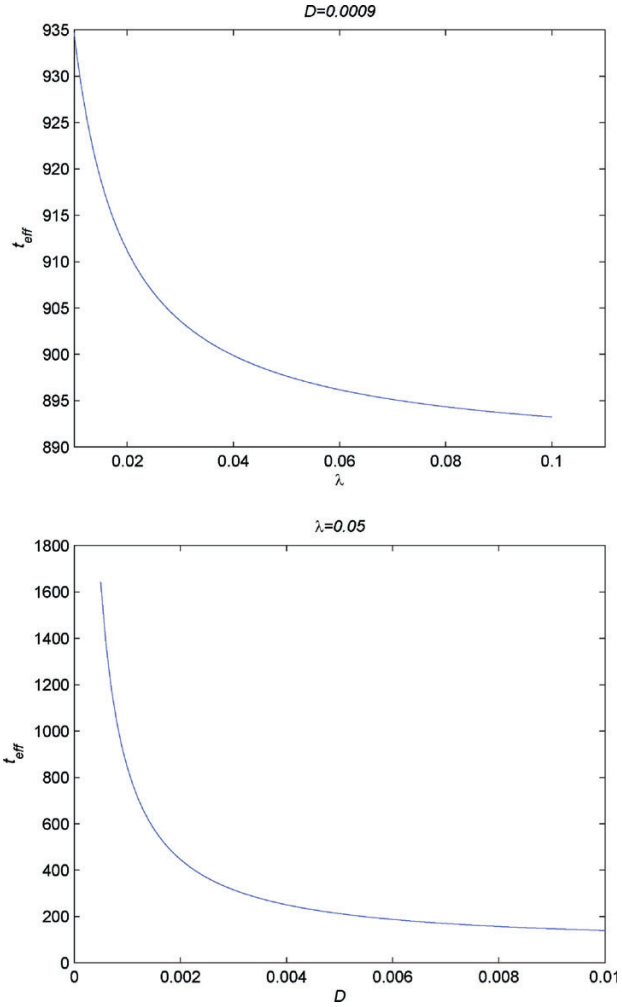

Fig. 6 – *Behavior of t_{eff} as a function of λ (left) and D (right)*

In engineering literature[22,23] it is generally accepted that the onset of equilibria is defined by the response time t_r, where $t_r = 4t_{eff}$.

If we compute $4t_{eff}$ for the previous systems, for $D = 0.05$, $l = 1$, $\lambda = 0.05$, $C^{0g} = 0.5$, $C^{0b} = 0.5$, $C^E = 0$, we obtain the values presented in Table 2.

Table 2 – *Response times of model I*

	System 1	System 2	System 3	System 4
$4t_{eff}$	32	121.6	116.5716	104

We note that $t_r^1 < t_r^4 < t_r^3 < t_r^2$, where the superscript refers to the systems. This result agrees with the inequalities established in (6) for the delivered masses. In fact as $M_2(t) < M_3(t)$ than the steady state of System 2 is reached after the steady state of System 3, that is $t_r^3 < t_r^2$. We observe that System 2 induces the largest delay. However it can not be used as a platform of drug delivery because the loading of particles still presents many laboratorial problems.

Interpreting t as a statistical variable, with exponential density distribution $d^*(t)$, the probability that $t \le kt_{eff}$, $P(t \le kt_{eff})$, is defined, for every $k \in \mathbb{R}$, by

$$P(t \le kt_{eff}) = 1 - e^{-k}.$$

As this probability can be viewed as $\frac{M_{est}(t)}{M^s}$, we have

$$M_{est}(t) = \left(1 - e^{-\frac{t}{t_{eff}}}\right) M^s, \qquad (13)$$

where $M_{est}(t)$ represents an estimation for $M(t)$.

Using the Final Value Theorem, $M^s = \lim_{p \to 0} p\overline{M}(p)$, we obtain

$$M^s = -2l(2C^E - C^{0g} - C^{0b}). \qquad (14)$$

An estimation $M_{est}(t)$ for the mass delivered during $[0, t]$, is defined by[23]

$$M_{est}(t) = -2l\left(1 - e^{-\frac{t}{t_{eff}}}\right)(2C^E - C^{0g} - C^{0b}). \qquad (15)$$

We observe that this estimation avoids the numerical solution of (1). It can be used with (10) as a simple tool to estimate the mass released until a certain time.

In Table 3 the estimated masses for several times t, computed using (13), are presented.

Table 3 – *Estimated delivery masses.*

t	$M_{est}(t)$
t_{eff}	63.21% M^s
$2t_{eff}$	86.47% M^s
$3t_{eff}$	95.02% M^s
$4t_{eff}$	98.17% M^s

In Table 4 are presented the estimated delivered masses $M_{est}(t)$, (15), and $M_3(t)$, (5), computed with $D = 0.05$, $l = 1$, $\lambda = 0.05$, $C^{0g} = 0.5$, $C^{0b} = 0.5$, $C^E = 0$.

The plots of the released mass $M_3(t)$ and the corresponding estimated mass $M_{est}(t)$ for the parameters in Table 4, are represented in Figure 7. The values of $M_3(t)$ have been computed from (5) with 100 terms. As expected when t increases a better approximation $M_{est}(t)$ of $M_3(t)$ is obtained.

Table 4 – *Estimated mass and total delivered mass for the therapeutical lens (Model I – System 3) ($D = 0.05$, $l = 1$, $\lambda = 0.05$, $C^{0g} = 0.5$, $C^{0b} = 0.5$, $C^E = 0$).*

Effective Time	Estimated Mass $M_{est}(t)$	Mass $M_3(t)$	Relative Error
$t_{eff} = 29.15$	63,21% $M^s = 1.2642$	1.4306919	1.320×10^{-1}
$2t_{eff} = 58.29$	86.47% $M^s = 1.7294$	1.7825530	3.073×10^{-2}
$3t_{eff} = 87.43$	95.02% $M^s = 1.9004$	1.9145475	7.445×10^{-3}
$4t_{eff} = 116.57$	98.17% $M^s = 1.9634$	1.9645691	5.954×10^{-4}

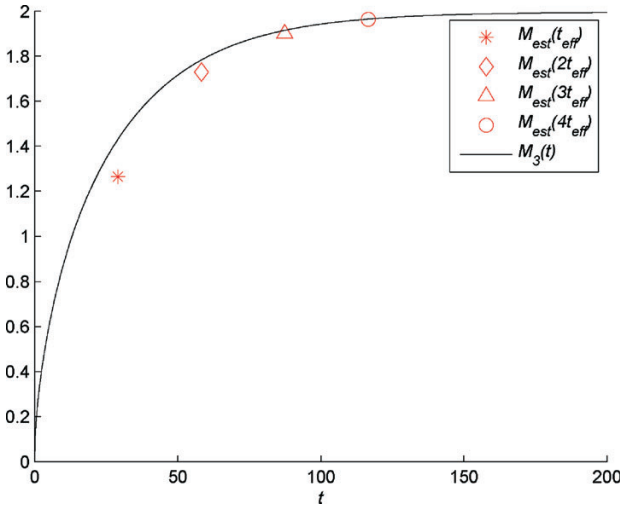

Fig. 7 – *Mass tracking of $M_3(t)$, for parameters in Table 3*

Once fixed a certain therapeutic mass and a certain waiting time to reach this mass, the lens can be tailored in order to fullfil these requirements. Let us consider, for example, that D and C^{0g} are free parameters. If we define that at $t_{eff} = 1000$, the released mass should be $M_{est}(4t_{eff}) = 1$, then

$$C^{0g} = 0.484329,\ D = 8.415 \times 10^{-3},$$

where $C^{0b} = 0.025$, $C^E = 0$, $l = 1$, $\lambda = 0.01$. If the same therapeutic mass is to be delivered within a shorter period of time, $t_{eff} = 100$, then as expected the diffusion coefficient increases, obtaining in this case $D = 1.774 \times 10^{-2}$. The change in drug delivery coefficient can be achieved by manipulating the polymer structure.

Numerical simulations versus experimental results

To manipulate analytically the equations in model (1) the diffusion coefficient was considered constant. As suggested by laboratorial experiments a more realistic model must include the concentra-

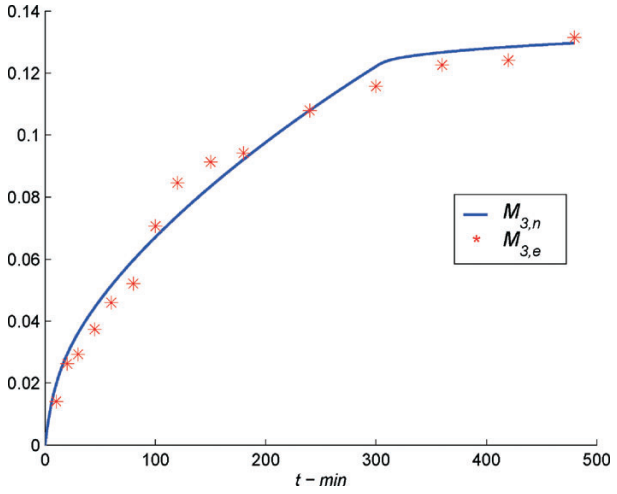

F i g . 8 – *Numerical ($M_{3,n}$) and experimental ($M_{3,e}$) mass delivered from a lens with dispersed drug and entrapped particles loaded with drug (System 3) during the first 8 hours*

tion dependence of the diffusion coefficient D, represented through a time dependence.

In Figure 8 we present the numerical released masses from System 3 – the lens with particles – and the experimental masses for the first eight hours. In the computations the following values of the parameters were considered:

$$C^{0b} = 0.05102,\ C^{0g} = 0.28,$$
$$\alpha_1 = 0.01,\ \lambda = 0.02 \tag{16}$$

and

$$D(t) = \begin{cases} 0.1996 \times 10^{-3}, & t \in [0,300], \\ 0.11 \times 10^{-4}, & t \in (300,\ 480]. \end{cases} \tag{17}$$

In Figure 9 we plot the results obtained from System 3 using experimental values and numerical

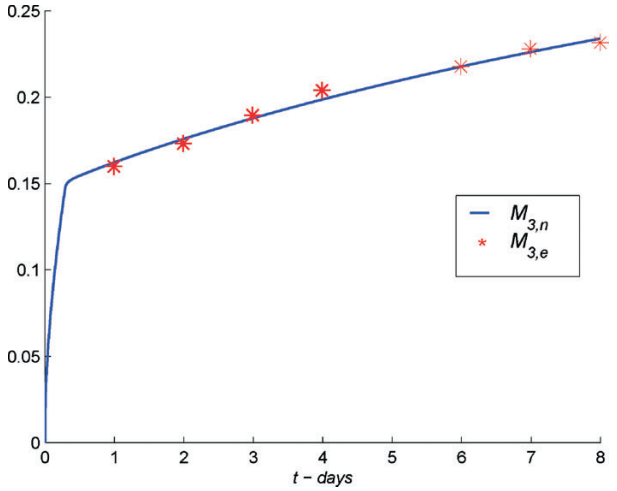

F i g . 9 – *Comparison of delivered numerical ($M_{3,n}$) and experimental ($M_{3,e}$) masses for System 3*

simulations for a period of eight days, where the diffusion is defined by

$$D(t) = \begin{cases} 0.1996 \times 10^{-3}, & t \in [0,420] \\ 0.9 \times 10^{-4}, & t \in (420,\ 11520] \end{cases}. \tag{18}$$

We note that expressions (17) and (18) correspond to diffusion coefficients measured in laboratory. To represent more realistically the exterior concentration we defined $C^E(t) = \gamma_1 u(-l, t)$ with $\gamma_1 = 0.5$.

A sandwich type lens

A different mechanism to induce delay in drug delivery from therapeutic lenses is to entrap the drug between polymeric layers.[15] The idea lies in creating sandwich type structures composed by three polymeric layers as represented in Figure 1: two non biodegradable layers (HEMA) coating a biodegradable PLGA film containing drug (Model II). As no analytical manipulations were carried on, diffusion coefficients have been represented by more realistically non linear functions.

Mathematical models

The behavior of the drug release is modeled by the coupled diffusion-reaction system of partial differential equations:

HEMA layer

$$\begin{cases} \dfrac{\partial C^1}{\partial t} = \dfrac{\partial}{\partial x}\left(D_1(C^1)\dfrac{\partial C^1}{\partial x} \right), & x \in (0, l_1),\ \ t > 0 \\ C^1(x,0) = 0, & x \in (0,\ l_1) \\ D_1 \dfrac{\partial C^1}{\partial x}(0,\ t) = \alpha(C^1(0,t) - C^E), & t > 0 \\ D_2 \dfrac{\partial C^1}{\partial x}(l_1,\ t) = D_2 \dfrac{\partial C^0}{\partial x}(l_1, t), & t > 0 \end{cases}, \tag{19}$$

PLGA film

$$\begin{cases} \dfrac{\partial C^0}{\partial t} = \dfrac{\partial}{\partial x}\left(D_2 \dfrac{\partial C^0}{\partial x} \right) + c_0 \gamma e^{-\gamma t}, & x \in (l_1, l_2),\ t > 0 \\ C^0(x,0) = C_0^0, & x \in (l_1,\ l_2) \\ C^0(l_1, t) = \beta C^1(l_1, t), & t > 0 \\ D_2 \dfrac{\partial C^0}{\partial x}(l_2,\ t) = D_1 \dfrac{\partial C^2}{\partial x}(l_2, t), & t > 0 \end{cases}, \tag{20}$$

HEMA layer

$$\begin{cases} \dfrac{\partial C^2}{\partial t} = \dfrac{\partial}{\partial x}\left(D_1(C^2)\dfrac{\partial C^2}{\partial x} \right), & x \in (l_2, l_3),\ t > 0 \\ C^2(x,0) = 0, & x \in (l_2,\ l_3) \\ C^2(l_2, t) = \beta C^0(l_2, t), & t > 0 \\ -D_1 \dfrac{\partial C^2}{\partial x}(l_3,\ t) = \alpha(C^2(l_3, t) - C^E), & t > 0 \end{cases}, \tag{21}$$

where $D_1(C) = D_{1e}e^{\beta_1(1-C/C_0^0)}$ and $D_2(t) = D_{2e}e^{-\beta_2 e^{-\gamma t}}$.

In (19)-(21) C^1 and C^2 represent the drug concentration in the non biodegradable layers, C^0 represent the drug concentration in the biodegradable PLGA film, D_{1e} and D_{2e} stand for the initial diffusion coefficients in HEMA and PLGA, respectively. We note that l_i are the thicknesses of the different layers, C_0^0 and c_0 are the free and bound initial concentrations in PLGA, respectively. Parameters α and β are related with the flux conditions at the boundary and at the interfaces, respectively; β_1 and β_2 are positive parameters. We assume that binding is not significant in HEMA layers. We observe that in equation (20) the source term $c_0\gamma e^{-\gamma t}$ represents the contribution of bound drug as PLGA film degradates. Such term is proportional to the initial concentration of bound drug with a time dependent degradation rate represented by $\gamma e^{-\gamma t}$.

Experiments carried with different types of sandwich structure: two HEMA layers linked by a void space containing drug (Model III) have also been described.[15] The kinetics of the release can be described by equations (19), (21) and an evolution equation in the void space of type

$$\begin{cases} \dfrac{\partial C^{vs}}{\partial t} = -\dfrac{1}{\varepsilon}\left[D_1\dfrac{\partial C^1}{\partial x}(l_1,t) + D_1\dfrac{\partial C^2}{\partial x}(l_1+\varepsilon,t)\right], \\ \qquad\qquad x \in (l_1, l_2),\ t > 0 \\ C^{vs}(0) = C_0^{vs} \end{cases} \tag{22}$$

where C^{vs} represents the drug concentration in the void space, C_0^{vs} the initial concentration and $e = l_2 - l_1$ stands for thickness of the void space between the two HEMA layers.

In Table 5 we present the description of the three types of lens we have mentioned so far.

Table 5 – *Description of the models*

Models	Definition	Main equations
Model I – System 3	Lens with particles encapsulating drug	(1)
Model II	Lens of "sandwich" type	(19), (20), (21)
Model III	Lens of "sandwich" type with a void cavity	(19), (22), (21)

We note that model I (System 3) corresponds to the lens described in section 2.1. We present in Figure 10 the plots of the total released masses, corresponding to models I, II and III with boundary conditions of type (4) that simulate *in vitro* results.

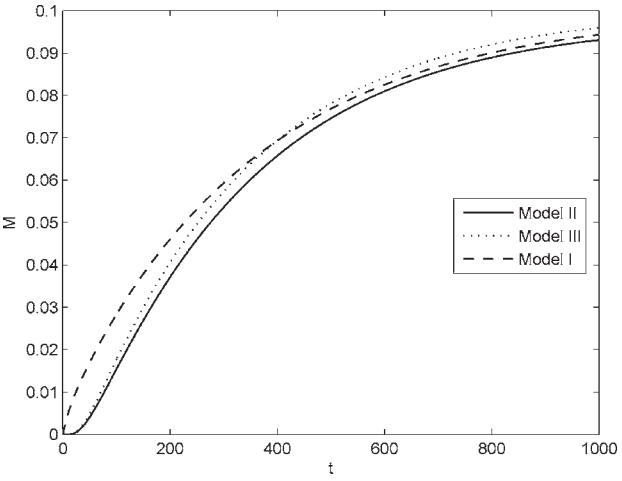

Fig. 10 – *Comparison of Models I, II and III*

Table 6 – *Parameters used in the simulations of Figure 10.*

Models	Parameters
Model I	$D = 0.005$, $\lambda = 0.05$, $C^{0b} = 0.01$, $C^{0g} = 0.04$, $l = 1$
Model II	$D_{1e} = 0.005$, $D_{2e} = 0.03$, $\beta_1 = 0.002$, $\beta_2 = 0.001$, $\gamma = 0.01$, $c_0 = 0.01$, $C_0^0 = 0.09$, $l_1 = l_2 = l_3 = 1$
Model III	$D_{1e} = 0.005$, $\beta_1 = 0.002$, $C_0^{vs} = 0.1$, $l_1 = l_3 = 1$

We considered $C^E = 0$, $\alpha = 0.01$, in all simulations and the values of the parameters exhibited in Table 6. If the drug is entrapped in a single non biodegradable layer where particles are dispersed (model I – System 3) the release is faster than in models II and III in a first period. Afterwards the plot corresponding to model III cross the plot of model I. We remark that "sandwich platforms" with a biodegradable layer – model II – lead to a slower drug release than "non sandwich platforms" – model I.

In Figure 11-up- we plot the total released mass of model II for two different degradation coefficients, and in Figure 11-down- we illustrate the behaviour of released mass for different free and bound initial concentration. In these simulations the following values were used: $C^E = 0$, $D_{1e} = 0.001$, $D_{2e} = 0.02$, $\alpha = 0.01$, $\beta_1 = 0.02$, $\beta_2 = 0.02$, $l_1 = l_2 = l_3 = 1$. From the figure in the top we conclude that the delivered mass is an increasing function of γ. In fact as the polymer erodes the bound drug is free to diffuse through the HEMA layers and the largest is the degradation rate the fastest is the release. The influence of initial concentration is also illustrated in the bottom of Figure 11: for each t the total released mass is a decreasing function of the initial bound mass. We observe that the values used for the parameters do not correspond to physical values.

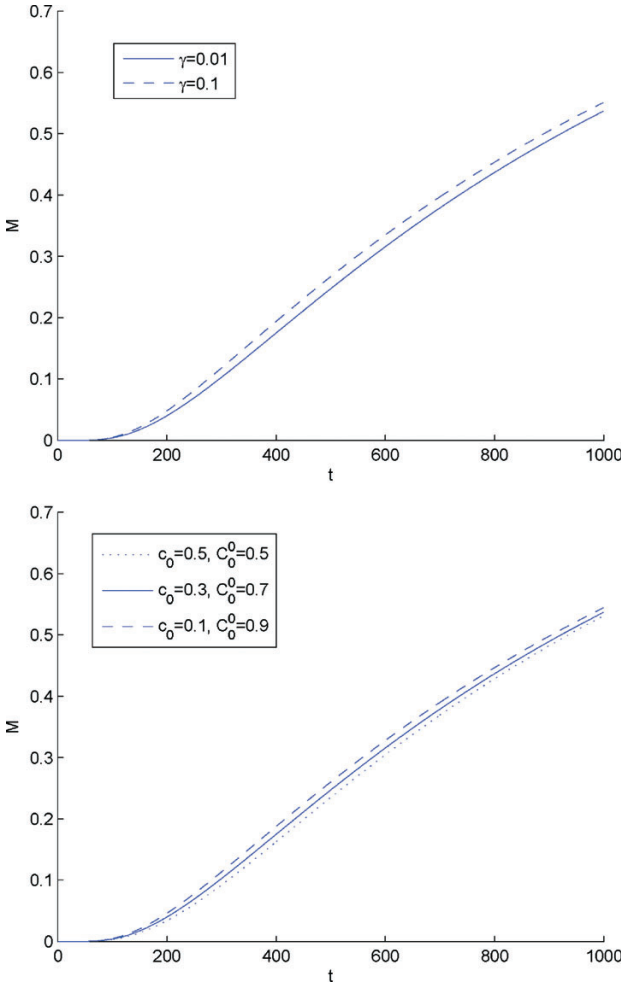

F i g . 1 1 – *A comparison of released mass from the "sandwich" lens (model II) for two different degradation coefficients* γ *(with* $c_0 = 0.3$, $C_0^0 = 0.7$*) -up- and different free and bound initial concentration -down- (with* $\gamma = 0.1$*)*

Numerical simulations versus experimental results

We compare now the numerical simulations obtained with model II with experimental results concerning the sandwich type lens under study. For this reason the mass units in this subsection are *mg*, as in the referred experimental paper.[15]

In Figure 12 numerical simulations of model II are compared with laboratorial results. We consider $C^E = 0$, $D_{1e} = 0.8554$, $D_{2e} = 4.2336 \times 10^{-7}$, $\alpha = 0.5$, $\beta_1 = 1.5$, $\beta_2 = 0.1$, $\gamma = 0.0714$, $c_0 = 0.03475$, $C_0^0 = 0.1$, $l_1 = 0.02$, $l_2 = 0.01$, $l_3 = 0.02$. The lens is still releasing drug after 30 days.[13] The qualitative behaviour of the numerical prediction shows a good agreement after day 5. We note that the experimental results exhibit an initial burst that is not present in the numerical solution. This is a point deserving some attention. In fact if there was no drug at all in the HEMA layers as reported in [13] this initial burst would not be expectable. This argument suggests

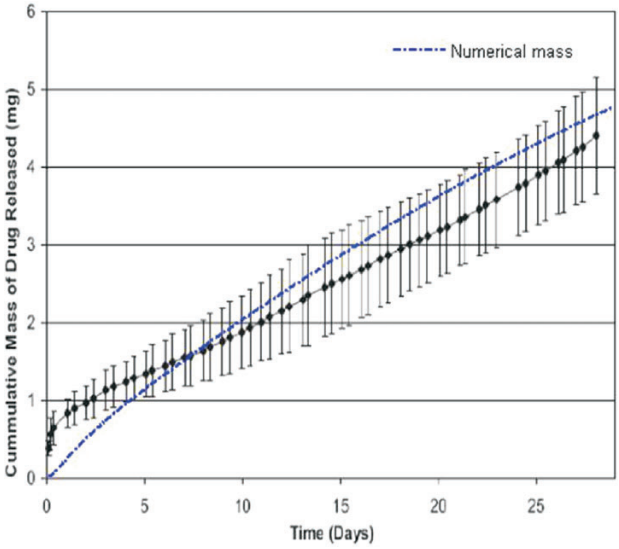

F i g . 1 2 – *Comparison of delivered numerical and experimental masses for "sandwich" type lens (model II)*

that the non biodegradable layers are not completely drug free. In fact, if we consider that $C^1(x, 0) \neq 0$, $x \in (0, l_1)$ and $C^2(x, 0) \neq 0$, $x \in (l_2, l_3)$ we obtain the result presented in Figure 13, where a numerical initial burst, agreeing with experimental results, is now observed.

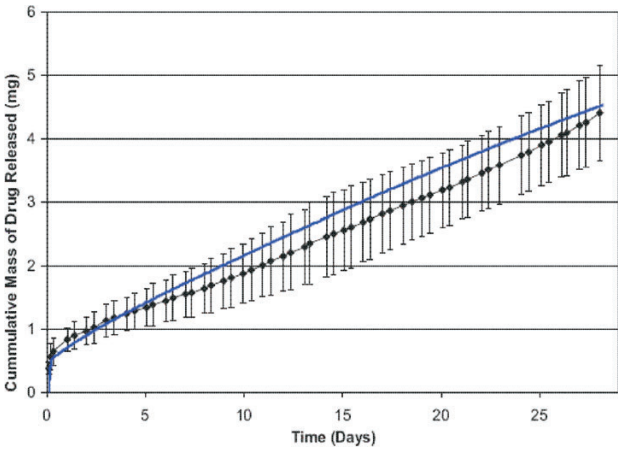

F i g . 1 3 – *Comparison of delivered numerical and experimental masses for "sandwich" type lens (model II)*

Simulating *in vivo* drug release from therapeutic lens

To have a prediction of the drug concentration in the anterior chamber of the eye we couple the systems representing the delivery from a therapeutic lens with the uptake in living tissues.

The eye is divided into anterior and posterior chamber (Figure 2). The anterior chamber is the

front portion of the eye containing aqueous fluid. It is bounded in front by the cornea and in the back by the iris and the lens. The posterior chamber is the space behind the iris, lens and ciliary body. In what follows the release from a therapeutic lens is compared with the behaviour of an instilled drop. The anatomy of the anterior chamber is included in the model and a pathological situation – the obstruction of Schlemm canals – is analyzed.

Diffusion in the cornea and anterior camera: therapeutic lens versus topical drops

We consider now the coupling of equations representing the diffusion in the lens, in the cornea and the evolution in the anterior chamber. In this model it is assumed that there is no convection of the aqueous humor. To model the diffusion of drug from a therapeutic lens through the cornea to the anterior chamber we consider equations (1) with $D = D_g$, in the domain $(-l_1, 0)$.

The behavior of the drug concentration in the cornea, C^c, is described by

$$\frac{\partial C^c}{\partial t} = D_c \frac{\partial^2 C^c}{\partial x^2} - K_c C^c, \quad x \in (0, l_2), \quad t > 0, \quad (23)$$

where D_c stands for the diffusion coefficient in the cornea and K_c represents a coefficient that takes into account the metabolic consumption.

The conservation of drug in the anterior chamber, C^a, is described by[17]

$$\frac{\mathrm{d}C^a}{\mathrm{d}t} = \frac{1}{V_a}\left(-D_c f_c A_c \frac{\partial C^c}{\partial x}(l_2, t) - Cl_a C^a(t)\right), \quad (24)$$

where A_c is the surface area of the cornea, f_c represents the fraction of A_c occupied by the diffusional route considered and V_a is the distribution volume of solute in the anterior chamber.

Equations (1), (23) and (24) are coupled with the initial conditions

$$C^g(x,0) = C^{0g}, \quad C^b(x,0) = C^{0b}, \quad x \in [-l_1, 0] \quad (25)$$

$$C^c(x,0) = 0, \quad x \in [0, l_1], \quad (26)$$

$$C^a(0) = 0, \quad (27)$$

and the boundary conditions

$$\frac{\partial C^g}{\partial x}(-l_1, t) = 0, \quad t > 0, \quad (28)$$

$$D_g f_g A_g \frac{\partial C^g}{\partial x}(0,t) = D_c f_c A_c \frac{\partial C^c}{\partial x}(0,t), \quad t > 0, \quad (29)$$

$$C^g(0,t) = K_{g,c} C^c(0,t), \quad t > 0, \quad (30)$$

$$-D_c f_c A_c \frac{\partial C^c}{\partial x}(l_2, t) = K_{c,a}(C^c(l_2,t) - C^a(t)), \quad t > 0. \quad (31)$$

In (29) f_g represents the fraction of the lens surface A_g that is occupied by the diffusional route. The constant $K_{g,c}$ (30) represents the quotient of the distribution coefficient in the lens and the cornea and the parameter $K_{c,a}$ represents a volumetric rate.

The dependence of C^a on the diffusion coefficient of the drug in the therapeutic lens is illustrated in Figure 14-up. As the drug diffusion coefficient in the lens increases, an increasing of the drug concentration in the anterior chamber is observed as expected.

An increasing of the drug clearance in the anterior chamber produces a decreasing of the drug concentration in this compartment. This behavior is illustrated in Figure 14-down.

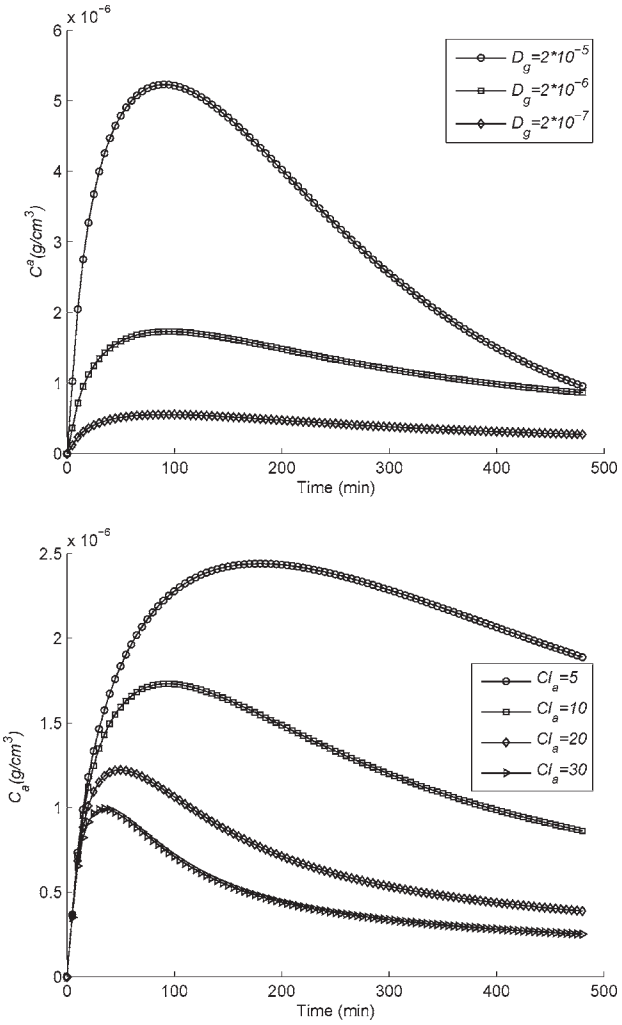

Fig. 14 – *Drug concentration in the anterior chamber C^a for different values of the diffusion coefficient in the lens (down) and for different values of the clearance in the anterior chamber (up).*

To compare the efficiency of therapeutic lens with topical eye drops we replaced the delivery from a therapeutical lens by equation

$$\frac{\mathrm{d}C_f}{\mathrm{d}t} = \frac{D_c f_c A_c \dfrac{\partial C^c}{\partial x}(0,t) - SC_f}{V_H + V_i e^{-K_d t}}, \quad (32)$$

where C_f denotes the drug concentration in the tear film and S represents a (fixed) lacrimal secretion rate. In (32) k_d denotes the drainage constant, V_L and V_i represent the normal lacrimal volume and the initial tear volume after an instillation of drug. The previous equation is coupled with the differential equations (2), (3), initial conditions (26), (27),

$$C_f(0) = C_f^0, \quad (33)$$

and with the boundary condition (31). The same assumption is considered in the mathematical model of topical administrations in some works found in the literature.[17,18] The coupling between the drug evolution in the tear film and in the cornea is defined by

$$-D_c f_c A_c \frac{\partial C^c}{\partial x}(0,t) = K_{c,a}(C_f(t) - C^c(0,t)). \quad (34)$$

In Figure 15 we plot the time evolution of drug concentration in the anterior chamber when a drop (C^a_{drop}) and a lens (C^a_{lens}) are used in drug administration. In the computation of $C^a_{drop}(t)$ the following parameters

$$k_d = 1.45,\ C_f^0 = 0.5 \text{ x } 10^{-3},\ V_L = 7,$$
$$V_i = 10,\ S = 1.2$$

are used.[17,18]

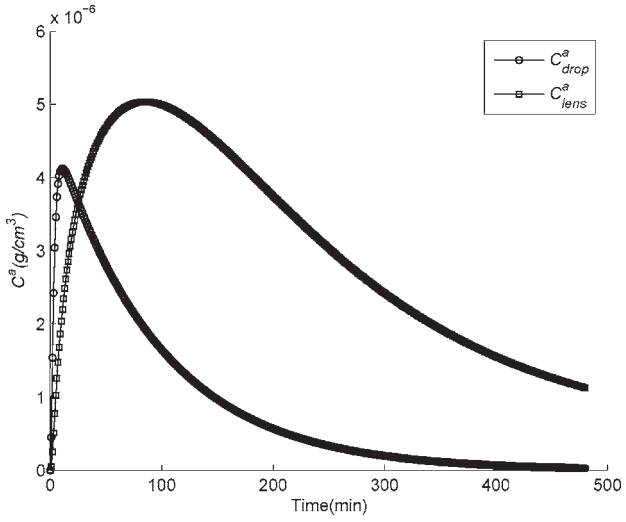

Fig. 15 – *Evolution of the drug concentration in the anterior chamber when a drop (C^a_{drop}) and a lenses (C^a_{lens}) are used in the eye drug administration*

From Figure 15 we conclude that the use of therapeutic lens leads to a higher concentration of the drug in the anterior chamber during a larger period of time than topical administrations. We observe that whereas using a therapeutic lens the drug concentration is significant after 8 hours, when a drop is instilled in the eye the drug concentration vanishes after some minutes.

Convective flow in the anterior chamber of the eye

In this section we describe very briefly the release of drug from a therapeutic lens, considering the convection of aqueous humour in the anterior chamber.[20] The anterior chamber is modeled using real dimensions. The domain is divided into three subdomains (see Figure 16): the therapeutic lens, Ω_1, where equations (1) hold; the cornea, Ω_2, where the drug concentration is described by (23); and the anterior chamber, Ω_3, where the convection-diffusion-reaction equation

$$\frac{\partial C_a}{\partial t} = D_a \Delta C_a - \vec{v} \cdot \nabla C_a - \frac{Cl_a}{V_a} C_a, \quad \Omega_3, \quad t > 0,$$

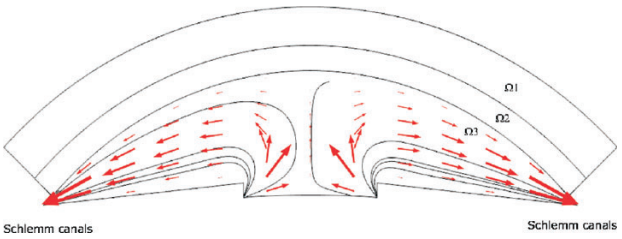

Fig. 16 – *Geometry of the therapeutical lens, cornea and anterior chamber*

is coupled with Navier Stokes equations. Initial, interface and boundary conditions complete the model. In (35) D_a denote the diffusion coefficient in the anterior chamber, $\vec{v}$ the velocity of the aqueous humour, Δ the Laplace operator and ∇ the gradient operator. As mentioned before the use of therapeutic lens is particulary important in the case of severe diseases characterized by high I.O.P.. The intraocular pressure can be explained by obstruction of Schlemm canals, (see Figure 2 and Figure 16) or high rates of aqueous humor production.

To simulate a pathological situation we consider a geometry with obstructed Schlemm canals. In our simulations this obstruction induces a high I.O.P. of mean value 30 *mmHg*, whereas a normal value lies in the interval [15,20]. To simulate the aqueous humour we considered an incompressible fluid ($\nabla \vec{v} = 0$) and we used the density and viscosity of water.

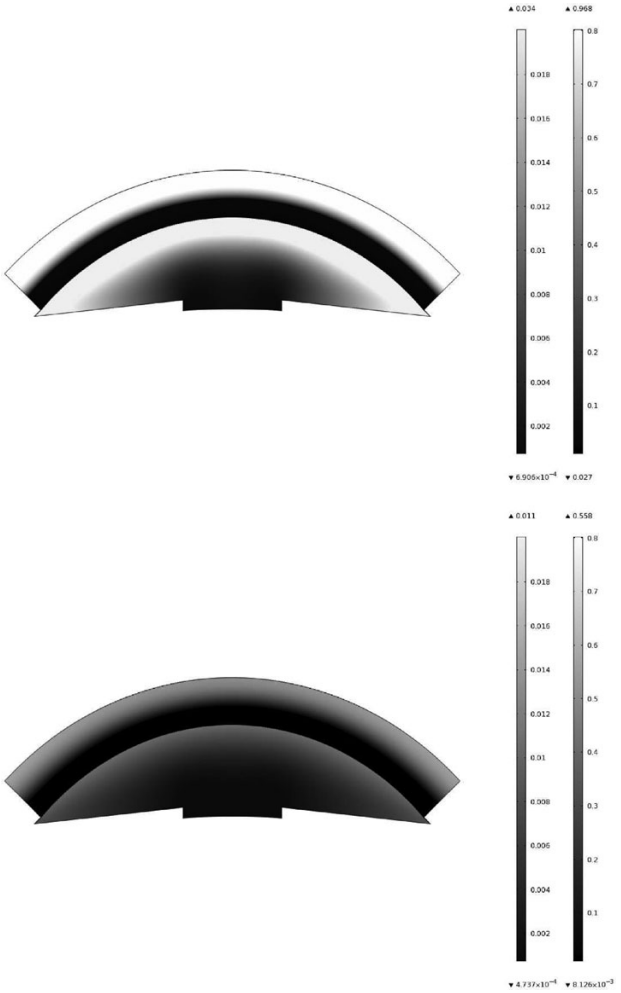

Fig. 17 – *Drug concentration at t = 20min – (top) and t = 2 h – (down)*

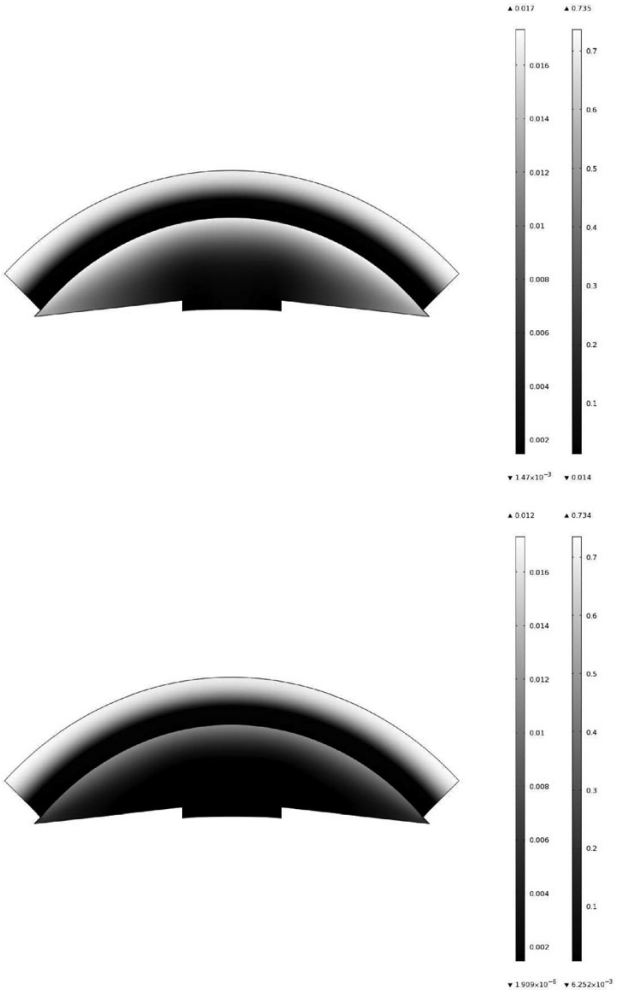

Fig. 18 – *Influence of the production rate on the distribution of drug concentration at t = 1 h*

In order to illustrate the evolution of drug concentration, we plot in Figure 17 its value at $t = 20$ *min* in (top) and at $t = 2$ *hour* in (down). Two types of gray scales have been used: a scale in the left for the concentration of drug in the lens and cornea and a scale in the right to represent the drug concentration in the anterior chamber. We note that, as defined in the scale, the lowest levels of drug concentration correspond to dark gray. When we compare these plots we can see that, as expected, the drug concentration decreases with time.

In Figure 18 we want to illustrate the influence of the production rate of the aqueous humour in the behaviour of drug concentration. We represent the drug concentration at $t = 1$ *h*, in the pathological situation described before; in Figure 18 – top – a normal rate was considered whereas in Figure 18 – down – the rate was doubled. We note that the increase in rate not only increases the I.O.P. (27,48 *mmHg* to 40,39 *mmHg*) but also leads to lowest values in drug concentration (see scale in Figure 18).

Conclusion

We presented in this paper an overview of controlled drug delivery from therapeutic lens to the anterior chamber of the eye. Mathematical models for *in vitro* delivery of different therapeutic lens were considered and numerical simulations were compared with laboratorial experiments. A time constant -effective time- was introduced and it was shown how it can be used as a tool to help in the design of therapeutic lens with predefined delivery profiles.

Mathematical models that represent *in vivo* delivery have also been considered. The effectiveness of controlled drug administration *versus* topical drops has been established.

To model pathologic situations – as the obstruction of Schlemm canals or an increase in the rate of production of aqueous humour – a more complex model[20] is introduced.

ACKNOWLEDGEMENTS

This research was supported by the Centre for Mathematics of the University of Coimbra and Fundação para a Ciência e a Tecnologia, through European program COMPETE/FEDER and by the FCT Research Project UTAustin/MAT/0066/2008.

Symbol

D – diffusion coefficient of the drug in the polymeric matrix (cm^2/min)
D_c – diffusion coefficient in the cornea (cm^2/min)
D_a – diffusion coefficient in the anterior chamber (cm^2/min)
C^g – drug concentration in the gel (g/cm^3)
C^b – drug concentration in the particles (g/cm^3)
λ – transfer coefficient (mm^{-1})
C^{0g} – initial concentration in the gel (g/cm^3)
C^{0g} – initial concentration in the particles (g/cm^3)
C^E – external concentration (g/cm^3)
α_1 – transference coefficient (cm/min)
M – exact solution for the total released mass (g)
M_i, i = 1,2,3,4 – represent the delivery mass for the Systems 1, 2, 3 and 4 (g)
$M_{3,n}$, $M_{3,e}$ – delivered numerical and experimental masses for System 3 (g)
γ_1 – rates distribution
C^1, C^2 – drug concentration in the non biodegradable layers (g/cm^3)
C^0 – drug concentration in the biodegradable layer (g/cm^3)
D_{1e}, D_{2e} – initial diffusion coefficients in HEMA and PLGA (cm^2/min)
l_i, i = 1,2,3 – thicknesses of the different layers (mm)
C_0^0, c_0 – free and bound initial concentrations in PLGA (g/cm^3)
α, β, β_1, β_2 – positive parameters
C^{vs} – the drug concentration in the void space in sandwich platform (g/cm^3)
C_0^{vs} – the initial concentration in the void space (g/cm^3)
C^c – drug concentration in the cornea (g/cm^3)
C^a – drug concentration in the anterior chamber (g/cm^3)
$K_{g,c}$ – quotient of the distribution coefficient in the lens and the cornea
$K_{c,a}$ – volumetric rate (cm^3/min)
K_c – metabolic consumption drug coefficient in the cornea
l_2 – cornea thickness (mm)
V_a – distribution volume of solute in the anterior chamber (μl)
Cl_a – clearance in the anterior chamber (μl/min)
A_c – surface area of the cornea (cm^2)
f_c – fraction of the cornea surface occupied by the diffusional route
C_f – drug concentration in the tear film (g/cm^3)
S – lacrimal secretion rate (μl/min)
k_d – drainage constant (min^{-1})
V_L – normal lacrimal volume in tear film (μl)
V_i – initial tear volume after an instillation of drug (μl)
C^a_{drop} – drug concentration in the anterior chamber when a drop is used (g/cm^3)
C^a_{lens} – drug concentration in the anterior chamber when a lens is used (g/cm^3)
v – velocity of the aqueous humour (mm/s)
$M_{est}(t)$ – estimated mass for $M(t)$
t_{eff} – effective time

References

1. *Grassi, M.*, CRC Press, (2006).
2. *Siepman, J., Siepman, F.*, International Journal of pharmaceutics. 364 Issue **2** (2008) 328.
3. *Bourlais, C. L., Acar, L., Zia, H., Sado, P.A., Needham, T., Leverge, R.*, Progress in Retinal Eye Research. **17** (1998) 33.
4. *Hehl, E.M., Beck, R., Luthard, K., Guthoff, R., Drewelow, B.*, European Journal of Clinical Pharmacology **55** (1999) 317.
5. *McNamara, N.A., Polse, K.A., Brand, R.J., Graham, A.D., Chan, J.S., Mckenney, C.D.*, American Journal of Ophthalmology. **127** (1999) 659.
6. *Nakada, K., Sugiyama, A.*, United States Patents. 6 **27** (1998) 745.
7. *Elisseeff, J., McIntosh, W., Anseth, K., Riley, S., Ragan, P., Langer, R.*, Journal of Biomedical Materials Research. **51** (2000) 164.
8. *Gulsen, D.; Chauhan, A.*, Investigative Ophthalmology and Visual Science. **45** (2004) 2342.
9. *Gulsen, D.; Chauhan, A.*, International Journal of Pharmaceutics. **292** (2005) 95.
10. *Ferreira, J. A., Oliveira, P., Silva, P. M., Carreira, A., Gil, H., Murta, J. N.*, Computer Modeling in Engineering and Science. **60** (2010) 152.
11. *Ferreira, J. A.; Oliveira, P.; Silva, P. M.; Murta, J. N.*, Computer Modeling in Engineering and Science. **71** (2011) 1.
12. *Podual, K., Doyle, F.J., Peppas, N. A.*, Polymer. **41** (2000) 3975.
13. *Scott, R. A., Peppas, N A.*, Biomaterials. **20** (1999) 1371.
14. *Silva, P.M.*, Phd-Thesis, University of Coimbra, Portugal, (2010).
15. *Ciolino, J. B., Hoare, T. R., Iwata, N. G., Behlau, I., Dohlman, C. H., Langer, R.; Kohane, D.S.*, Investigative Ophthalmology & Visual Science. **50** (2009) 3346.
16. *Ferreira, J. A., Oliveira, P., Silva, P. M.*, CMMSE 2011, Volume II, edt. J. Vigo Aguiar, (2011) 496.
17. *Avtar R., Tandon D.*, European Journal of Pharmaceutical Sciences. **35** (2008) 175.
18. *Zhang, W., Prausnitz, M.R., Edwards, A.*, Journal of Controlled Release. **99** (2004) 241.
19. *Worakula, N., Robinson, J.R.*, European Journal of Pharmaceutics and Biopharmaceutics. **44** (1997) 71.
20. *Ferreira, J. A., Oliveira, P., Silva, P. M.*, submited (2012).
21. *Collins, R.*, Journal Physics D: Applied Physics. **13** (1980) 1935.
22. *Simon, L.*, Mathematical Bioscience. **217** (2009) 151.
23. *Ferreira, J. A., Oliveira, P., Silva, P. M.*, Computer Modeling in Engineering and Science. **76** (2011) 164.